

# Assessment of epidermal growth factor receptor status in glioblastomas

Hui-Jun Zhu<sup>1</sup>, Mikako Ogawa<sup>2</sup>, Yasuhiro Magata<sup>2</sup>, Masahiko Hirata<sup>3</sup>, Yoshiro Ohmomo<sup>3</sup>, Hiroki Namba<sup>4</sup>, Harumi Sakahara\*<sup>1</sup>

<sup>1</sup> Department of Radiology, Hamamatsu University School of Medicine, Japan

<sup>2</sup> Medical Photonics Research Center, Hamamatsu University School of Medicine, Japan

<sup>3</sup> Osaka University of Pharmaceutical Sciences, Japan.

<sup>4</sup> Department of Neurosurgery, Hamamatsu University School of Medicine, Japan

## ARTICLE INFO

### Article type:

Original article

### Article history:

Received: 29-Apr-2013

Revised: 7-Jun-2013

Accepted: 16-Jun-2013

### Keywords:

[<sup>125</sup>I]PYK

Gefitinib

EGFR

Glioblastoma

## ABSTRACT

**Objective(s):** Our previous study showed that a newly designed tracer radioiodinated 6-(3-morpholinopropoxy)-7-ethoxy-4-(3'-iodophenoxy)quinazoline ([<sup>125</sup>I]PYK) is promising for the evaluation of the epidermal growth factor receptor (EGFR) status and prediction of gefitinib treatment of non-small cell lung cancer. EGFR is over-expressed and mutated also in glioblastoma. In the present study, the expressions and mutation of EGFR were tested with [<sup>125</sup>I] PYK in glioblastoma *in vitro* and *in vivo* to determine whether this could be used to predict the sensitivity of glioblastoma to gefitinib treatment.

**Methods:** Glioblastoma cell lines with different expression of EGFR were tested. Growth inhibition of cell lines by gefitinib was assessed by the 3-(4, 5-dimethylthiazol-2-yl)-2, 5-diphenyltetrazolium bromide (MTT) colorimetric assay. Uptake levels of [<sup>125</sup>I]PYK were evaluated in cell lines *in vitro*. Tumor targeting of [<sup>125</sup>I]PYK was examined by a biodistribution study and imaging by single photon emission computed tomography (SPECT).

**Results:** High concentrations of gefitinib were needed to suppress EGFR-mediated proliferation. The uptake of [<sup>125</sup>I] PYK in cell lines *in vitro* was low, and showed no correlation with EGFR expression or mutation status. Biodistribution study and SPECT imaging with [<sup>125</sup>I]PYK for xenografts showed no [<sup>125</sup>I]PYK uptake.

**Conclusion:** The results showed prediction of gefitinib effectiveness was difficult in glioblastoma by [<sup>125</sup>I]PYK, which might be due to the complicated expression of EGFR status in glioblastoma. Thus, new tracers for sites downstream of the mutant EGFR should be investigated in further studies.

### Please cite this paper as:

Zhu HJ, Ogawa M, Magata Y, Hirata M, Ohmomo Y, Namba H, Harumi S. Assessment of epidermal growth factor receptor status in glioblastomas. Asia Oceania J Nucl Med Biol. 2013; 1(2):47-52.

## Introduction

Glioblastoma multiforme (GBM) is the most common and highly aggressive malignant neoplasm of the central nervous system (CNS) (1). Despite the development of multi-treatment regimens, the treatment of glioblastomas remains difficult. Patients with GBM have a poor prognosis, with a median survival of

approximately 12 months (2). The abnormal alteration of epidermal growth factor receptor (EGFR) genes is associated with the progression of GBM. About 40% of primary GBM show amplification of the EGFR gene and subsequent elevated levels of EGFR protein (3). About 63% to 75% of GBM with EGFR over-expression have been found with mutation of the EGFR genes. The

\*Corresponding author: Harumi Sakahara, Department of Radiology, Hamamatsu University School of Medicine, 1-20-1 Handayama, Higashiku, Hamamatsu, Shizuoka 431-3192, Japan. TEL: +81-53-435-2240; FAX: +81-53-435-2241; E-mail: sakahara@hama-med.ac.jp

© 2013 mums.ac.ir All rights reserved.

This is an Open Access article distributed under the terms of the Creative Commons Attribution License (<http://creativecommons.org/licenses/by/3.0/>), which permits unrestricted use, distribution, and reproduction in any medium, provided the original work is properly cited.

aberrant EGFR alterations in GBM have been considered as novel targets for diagnostic, prognostic and therapeutic purposes (4).

Much effort has been expended in developing EGFR-targeted therapies. One promising approach is focused on epidermal growth factor receptor tyrosine kinase (EGFR TK) inhibitors. For example, gefitinib and erlotinib could competitively bind to the adenosine triphosphate (ATP)-binding pocket in the kinase domain (5). Some preclinical studies have also shown promise of the EGFR TK inhibitor for GBM (6). However, the objective response rate for GBM patients treated with EGFR TK inhibitors is only 10 to 20 percent in clinical trials (7, 8). Therefore, it is important that a new approach to characterize EGFR expression and mutation in individual GBM patients is developed.

Quantitative non-invasive molecular imaging might aid in developing EGFR TK inhibitors and in patient selection for EGFR TK inhibitors. Some radiolabeled agents for molecular imaging have been successfully used for detecting EGFR expression in non-small cell lung carcinomas (NSCLC) (9). However, there is a lack of studies on the detection of mutant EGFR genes in GBM. In our previous study, an EGFR molecular imaging tracer radioiodinated 6-(3-morpholinopropoxy)-7-ethoxy-4-(3'-iodophenoxy) quinazoline ( $[^{125}\text{I}]PYK$ ) was developed to detect EGFR expression and mutation. It predicted whether gefitinib would be effective in NSCLC, and we showed previously that the target tumor could be clearly visualized by  $[^{125}\text{I}]PYK$ -SPECT (10, 11). Now we present *in vivo* and *in vitro* studies of  $[^{125}\text{I}]PYK$  aimed at detecting EGFR expression status in GBM.

## Materials and Methods

### *Radiolabeling of PYK*

$[^{125}\text{I}]NaI$  was obtained from MP Biomedicals Japan (Tokyo, Japan).  $[^{125}\text{I}]PYK$  was synthesized according to the method previously reported using  $[^{125}\text{I}]NaI$  (10). Briefly, aqueous hydrogen peroxide (10  $\mu\text{L}$ , 30%) was added to a mixture of  $[^{125}\text{I}]NaI$  (10  $\mu\text{L}$ , 37.0 MBq, 74 TBq/mmol), 0.1 M HCl (25  $\mu\text{L}$ ) and the tributylstannyl precursor of PYK (0.01 mg in 10  $\mu\text{L}$  ethanol). After 10 min reaction,  $[^{125}\text{I}]PYK$  was purified by HPLC. Radiochemical yield was 97.5%, and radiochemical purity was more than 95%.

### *Cells*

The human glioblastoma cell lines were kindly provided by Professor Motoo Nagane. U87MG, U87MG. $\Delta$ EGFR, U87MG.wtEGFR, and U87MG.DK used in this study were described previously (12). These cells showed the following different EGFR

expressions: U87MG expresses a low amount of wild-type EGFR; U87MG. $\Delta$ EGFR overexpresses the type III deletion-mutant gene for EGFR; U87MG.DK expresses a kinase-deficient mutant of  $\Delta$ EGFR; and U87MG.wtEGFR expresses exogenous wild type (wt) EGFR (12). Human epithelial carcinoma cell line A431 with a high expression of EGFR, was used as the positive control. Cell lines were routinely cultured in DMEM supplemented with 10% fetal bovine serum and were maintained at 37 °C in a humidified 95% air - 5% CO<sub>2</sub> atmosphere.

### *Binding specificity of $[^{125}\text{I}]PYK$ to glioblastoma cells*

Gefitinib was purchased from Cayman chemical (Michigan, USA). Competitive inhibition experiments were carried out in order to test the specificity of the compound in inhibiting EGFR. Cells were grown in 6-well plates and pretreated by 10  $\mu\text{M}$  gefitinib for 10 min at 37 °C. Then 0.74 kBq  $[^{125}\text{I}]PYK$  was added to the a cell suspension of  $1.0 \times 10^6$  cells in 1 mL PBS. The radioactivity incorporated in the cells was determined on a gamma counter.

### *Inhibition of tumor cell growth by gefitinib in vitro*

Growth inhibition was assessed using 3-(4,5-dimethylthiazol-2-yl)-2, 5-diphenyltetrazolium bromide (MTT) colorimetric assay. Cells were seeded at 5000 per well in 96-well plates. Cells were treated with various concentrations of gefitinib (0.05-20  $\mu\text{mol/L}$ ) for 72 hr at 37 °C, followed by incubation for 2 hr at 37 °C with 10 mg/mL MTT. The results were determined by measuring the optical density of cell lysates at a wavelength of 570 nm. The IC<sub>50</sub> values were defined as the concentration of gefitinib needed for a 50% reduction based on cell growth curves.

### *Xenografts model*

Approximately  $1 \times 10^6$  glioblastoma cells in phosphate-buffered saline (PBS) were injected subcutaneously into the flanks of 4- to 6-wk-old female BALB/c nude mice. Tumor volumes were measured by the formula (length $\times$ width<sup>2</sup>)  $\times 0.5$ .

### *Biodistribution study of $[^{125}\text{I}]PYK$*

Nude mice (n=4) with xenograft tumors received tail vein injections of 37 kBq of  $[^{125}\text{I}]PYK$  in 0.1 mL of saline for biodistribution study. At 24 hr after injection, blood, lung, muscle, heart, spleen, stomach, small intestine, kidney, liver and tumor samples were collected and weighed, and radioactivity was assayed in a gamma counter. The results were calculated as percentages of injected dose (ID) per gram of tissue.

### Imaging of nude mice with xenografts with SPECT

Nude mice (n=4) bearing U87MG.  $\Delta$ EGFR xenograft underwent single photon emission computed tomography (SPECT) scans when the tumor volume reached 300–400 mm<sup>3</sup>. The mice were injected with 12.95 MBq of [<sup>125</sup>I]PYK and imaged on the Micro-PET/SPECT/CT scanner (Gamma Medica-Ideas, Inc., Northridge, CA). The scans were performed at 1, 3 and 24 hr after injection.

## Results

### Binding specificity of [<sup>125</sup>I]PYK to glioblastoma cells

The binding of [<sup>125</sup>I]PYK to glioblastoma cells was inhibited by pretreatment with gefitinib (Figure 1). The specific binding of [<sup>125</sup>I]PYK, however, was similar in all cell lines, and there was no correlation with EGFR expression and mutation.

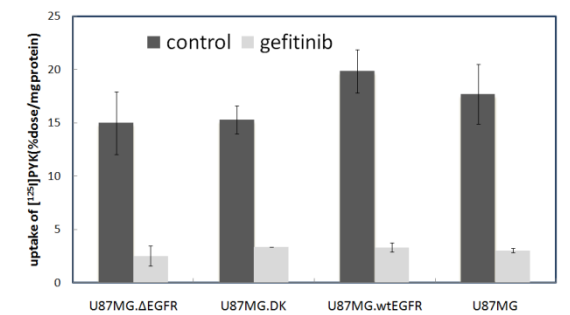


**Figure 1.** Decreased uptake of [<sup>125</sup>I]PYK by cultured cells after treatment with gefitinib, data represent mean  $\pm$  SD, n = 3.

### Inhibition of tumor cell growth by gefitinib *in vitro*

MTT assay showed U87 cell lines had similar sensitivities to gefitinib in each other, but required higher doses of gefitinib compared with representative gefitinib-sensitive A431 cell lines (Table 1).

**Table 1.** The cell growth and EGFR TK activities inhibition of U87 cell lines by gefitinib

Cell lines	IC <sub>50</sub> ( $\mu$ M)
A431	0.31 $\pm$ 0.09
U87MG.ΔEGFR	15.3 $\pm$ 0.3
U87MG.DK	16.7 $\pm$ 1.9
U87MG.wtEGFR	26.7 $\pm$ 1.3
U87MG	14.2 $\pm$ 1.6

Cells were measured after a 72 hr incubation of gefitinib, assays for all cell lines were performed in triplicate

### Biodistribution of [<sup>125</sup>I]PYK in nude mice

The biodistribution properties of [<sup>125</sup>I]PYK are shown in Table 2. The distributions of [<sup>125</sup>I]PYK

in tumors and organs were evaluated at 24 hr post injection. Normal organ uptake of radioactivity was highest in colon. High tumor/muscle and tumor/blood ratios were observed in all cell lines. However, the accumulated radioactivity in the tumor was not high enough for *in vivo* tumor detection.

### In vivo SPECT/CT Imaging with [<sup>125</sup>I]PYK

In nude mice (n=4) bearing xenografts of U87MG.ΔEGFR cells SPECT/CT imaging was performed at 1 hr, 3 hr and 24 hr post injection. High activity accumulations were visualized in the liver and colon at 1 hr and 3 hr, followed thereafter by decline, showing the clearance pathway of the [<sup>125</sup>I]PYK. Tumors could not be detected by [<sup>125</sup>I]PYK in 24 hr imaging (Figure 2).

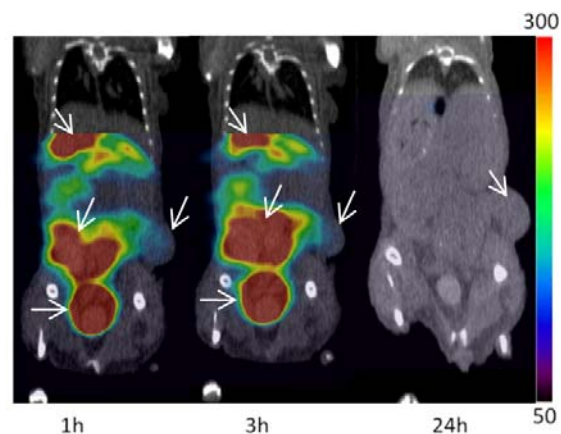


**Figure 2.** SPECT/CT image of [<sup>125</sup>I]PYK in U87MG.ΔEGFR xenograft at 1 hr, 3 hr, 24 hr post injection. The colon, liver, bladder and tumor were indicated by arrows. The thyroid was out of field of view in these SPECT images.

## Discussion

Although gefitinib treatment is promising for many kinds of tumors depending on EGFR expression (13–15), its application as an effective therapy for GBM remains to be established (16). It was previously shown that NSCLC patients who had specific EGFR gene mutations, especially in-frame deletions in exon 19 ( $\Delta$ LRE) and a point mutation in exon 21 (L858R), could benefit from gefitinib (17). These mutations, however, have rarely been reported in gliomas. The most frequent mutation in gliomas is the  $\Delta$ EGFR mutation with the loss of exons 2 to 7 of the EGFR gene, resulting in an in-frame deletion of 267 amino acids in the extracellular domain (18). Although  $\Delta$ EGFR is unable to bind to EGF, it is still constitutively phosphorylated and activates downstream signaling cascades, and promotes the survival and proliferation of glioblastoma cells (19).  $\Delta$ EGFR may sensitize glioblastoma cells to EGFR kinase inhibitors by promoting chronic

**Table 2.** Biodistribution of [<sup>125</sup>I]PYK in nude mice at 24h post-injection (%ID/g)<sup>a</sup>

Tissue	xenograft of cell lines			
	U87MG.ΔEGFR	U87MG.DK	U87MG.wtEGFR	U87MG
Tumor	0.17 ± 0.06	0.24 ± 0.16	0.18 ± 0.07	0.15 ± 0.02
Blood	0.05 ± 0.01	0.05 ± 0.00	0.05 ± 0.01	0.05 ± 0.01
Pancreas	0.06 ± 0.03	0.20 ± 0.02	0.15 ± 0.04	0.21 ± 0.02
Spleen	0.12 ± 0.00	0.16 ± 0.01	0.13 ± 0.01	0.17 ± 0.03
Stomach	0.62 ± 0.56	0.38 ± 0.54	0.54 ± 0.47	0.64 ± 0.80
Small intestine	0.59 ± 0.28	0.87 ± 0.13	0.79 ± 0.52	1.01 ± 0.23
Colon	1.69 ± 0.41	5.32 ± 1.22	3.26 ± 1.49	5.57 ± 0.96
Liver	0.42 ± 0.14	0.47 ± 0.05	0.48 ± 0.12	0.55 ± 0.09
Kidney	0.30 ± 0.05	0.32 ± 0.03	0.25 ± 0.04	0.34 ± 0.02
Heart	0.09 ± 0.02	0.11 ± 0.01	0.08 ± 0.01	0.09 ± 0.01
Lung	0.17 ± 0.04	0.21 ± 0.08	0.16 ± 0.01	0.22 ± 0.03
Brain	0.03 ± 0.01	0.03 ± 0.00	0.02 ± 0.01	0.03 ± 0.01
Muscle	0.05 ± 0.01	0.08 ± 0.05	0.06 ± 0.02	0.07 ± 0.01
Bone	0.31 ± 0.07	0.32 ± 0.05	0.36 ± 0.15	0.37 ± 0.15
Uptake ratio <sup>b</sup>				
Brain/Blood	0.64 ± 0.17	0.56 ± 0.03	0.48 ± 0.17	0.61 ± 0.13
Tumor/Muscle	3.78 ± 1.09	4.23 ± 3.47	3.29 ± 1.83	2.16 ± 0.33
Tumor/Blood	3.90 ± 1.67	4.71 ± 3.25	3.89 ± 1.67	2.95 ± 0.60

a) The data are expressed as Mean % injection dose ± S.D. per gram, n=4.

b) Ratio of brain to blood or tumor-to-normal tissue.

dependence on phosphoinositide-3 kinase (PI3K) signaling. Some reports have shown the prognostic value of ΔEGFR mutation for TK inhibitor treatment and therefore suggested it as a target for cancer therapeutics (8, 20).

Previous studies have successfully shown through non-invasive imaging of EGFR expression, that the mutation status in NSCLC could aid in the selection of patients for individualized therapy with EGFR kinase inhibitors (21). However, the *in vivo* detection of EGFR expression and mutation in GBM, has been more difficult. Our study explored the use of [<sup>125</sup>I]PYK as a potential probe for detection of EGFR mutations in xenografts of U87 glioblastoma cells in mice to predict treatment with gefitinib treatment. In our previous study, we successfully imaged the EGFR mutation in NSCLC with [<sup>125</sup>I]PYK (10, 11). The biodistribution experiments demonstrated that the blood radioactivity was 0.80% of the injected dose per mL at 1hr and decreased to 0.03% of the injected dose per mL at 24 hr. Although the tumor uptake decreased from 4.37% of the injected dose per gram (%ID/g) at 1 hr to 1.53%

of the injected dose per gram (%ID/g) at 24 hr, the tumor-to-blood radioactivity ratio increased at 24 hr after injection (10, 11). Based on these results, we examined the biodistribution at 24 hr after the injection in the present study. We did not examine the stability of [<sup>125</sup>I]PYK *in vitro* nor measured thyroid uptake in mice after the injection of [<sup>125</sup>I]PYK. In the previous study, however, the uptake in the stomach at 1 hr post-injection was 6.10% of the injected dose per gram (%ID/g) and lower than in the liver of 27.0% of the injected dose per gram (%ID/g) and in the kidneys of 7.40% of the injected dose per gram (%ID/g). The uptake in the stomach decreased promptly. The thyroid could not be detected by SPECT imaging (10). Even if iodine may release from the compound, it is likely that de-iodination is not significant in this compound.

In gliomas over-expressing ΔEGFR with high phosphorylation activity, *in vivo* imaging showed no specific uptake in tumors. The differences in results of *in vivo* imaging in NSCLC and in gliomas might be due to the different genetic alterations of EGFR observed in gliomas although a previous study suggested that U87 cells were very

sensitive to the EGFR inhibitor (22). The molecular mechanism determining the binding of 4-quinazoline compounds may be different as observed in NSCLC and therefore, needs to be more thoroughly investigated. In gliomas, clinical response requires sufficient plasma concentrations of EGFR tyrosine kinase inhibitor to abrogate downstream signaling (17). Also, cross-talk pathways of ΔEGFR and coactivation of EGFR TKs have been found frequently in GBMs (23), which might influence [<sup>125</sup>I]PYK specific binding to EGFR.

In conclusion, the failure of detection of EGFR expression in GBM, might be due to the complicated expression of EGFR status in GBM, suggesting that prediction of gefitinib effectiveness is difficult in GBM. As the activation and aberrant behavior downstream have been considered as new checkpoints for forecasting the results of TK inhibitor regimens, our further study will aim at developing radiolabeled agents for detecting the downstream pathway of EGFR.

## References

- Maher EA, Furnari FB, Bachoo RM, Rowitch DH, Louis DN, Cavenee WK, et al. Malignant glioma: genetics and biology of a grave matter. *Genes Dev.* 2001; 15: 1311-33.
- Stupp R, Hegi ME, van den Bent MJ, Mason WP, Weller M, Mirimanoff RO, et al. Changing paradigms an update on the multidisciplinary management of malignant glioma. *Oncologist.* 2006; 11: 165-80.
- Cancer Genome Atlas Research Network. Comprehensive genomic characterization defines human glioblastoma genes and core pathways. *Nature.* 2008; 455: 1061-8.
- Parsons DW, Jones S, Zhang X, Lin JC, Leary RJ, Angenendt P, et al. An integrated genomic analysis of human glioblastoma multiforme. *Science.* 2008; 321: 1807-12.
- Wakeling AE, Guy SP, Woodburn JR, Ashton SE, Curry BJ, Barker AJ, et al. ZD1839 (Iressa) an orally active inhibitor of epidermal growth factor signaling with potential for cancer therapy. *Cancer Res.* 2002; 62, 5749-54.
- Mellinghoff IK, Cloughesy TF, Mischel PS. PTEN-mediated resistance to epidermal growth factor receptor kinase inhibitors. *Clin Cancer Res.* 2007; 13: 378-81.
- Franceschi E, Cavallo G, Lonardi S, Magrini E, Tosoni A, Grosso D, et al. Gefitinib in patients with progressive high-grade gliomas: a multicentre phase II study by Gruppo Italiano Cooperativo di Neuro-Oncologia (GICNO). *Br J Cancer.* 2007; 96: 1047-51.
- Mellinghoff IK, Wang MY, Vivanco I, Haas-Kogan DA, Zhu S, Dia EQ, et al. Molecular determinants of the response of glioblastomas to EGFR kinase inhibitors. *N Engl J Med.* 2005; 353: 2012-24.
- Liu N, Li M, Li X, Meng X, Yang G, Zhao S, et al. PET-based biodistribution and radiation dosimetry of epidermal growth factor receptor-selective tracer <sup>11</sup>C-PD153035 in humans. *J Nucl Med.* 2009; 50: 303-8.
- Hirata M, Kanai Y, Naka S, Yoshimoto M, Kagawa S, Matsumuro K, et al. A useful EGFR-TK ligand for tumor diagnosis with SPECT: development of radioiodinated 6-(3-Morpholinopropoxy)-7-ethoxy-4-(3-iodophenoxy)quinazoline. *Ann Nucl Med.* 2013; 27: 431-43.
- Yoshimoto M, Hirata M, Magata Y, Nishii R, Kawai K, Ohmomo Y. Evaluation of radioiodinated PYK for monitoring active mutation of EGFR-TK. *J Nucl Med.* 2012; 53: (Supplement 1): 1657.
- Nagane M, Levitzki A, Gazit A, Cavenee WK, Huang HJ. Drug resistance of human glioblastoma cells conferred by a tumor-specific mutant epidermal growth factor receptor through modulation of Bcl-XL and caspase-3-like proteases. *Proc Natl Acad Sci U S A.* 1998; 95: 5724-9.
- Lorusso PM. Phase I studies of ZD1839 in patients with common solid tumors. *Semin Oncol.* 2003; 30: 21-9.
- Sordella R, Bell DW, Haber DA, Settleman J. Gefitinib-sensitizing EGFR mutations in lung cancer activate anti-apoptotic pathways. *Science.* 2004; 305: 1163-7.
- Watanabe S, Tanaka J, Ota T, Kondo R, Tanaka H, Kagamu H, et al. Clinical responses to EGFR-tyrosine kinase inhibitor retreatment in non-small cell lung cancer patients who benefited from prior effective gefitinib therapy: a retrospective analysis. *BMC cancer.* 2011; 11: 1.
- Rich JN, Reardon DA, Peery T, Dowell JM, Quinn JA, Penne KL, et al. Phase II trial of gefitinib in recurrent glioblastoma. *J Clin Oncol.* 2004; 22: 133-42.
- Lynch TJ, Bell DW, Sordella R, Gurubhagavatula S, Okimoto RA, Brannigan BW, et al. Activating mutations in the epidermal growth factor receptor underlying responsiveness of non-small-cell lung cancer to gefitinib. *N Engl J Med.* 2004; 350: 2129-39.
- Johns TG, Perera RM, Vernes SC, Vitali AA, Cao DX, Cavenee WK, et al. The Efficacy of epidermal growth factor receptor-specific antibodies against glioma xenografts Is influenced by receptor levels, activation Status, and heterodimerization. *Clin Cancer*

- Res. 2007; 13: 1911-25.
19. Lemmon MA, Schlessinger J. Cell signaling by receptor tyrosine kinases. *Cell*. 2010; 141: 1117-34.
  20. Weinstein IB, Joe AK. Mechanisms of disease: Oncogene addiction-a rationale for molecular targeting in cancer therapy. *Nat Clin Pract Oncol*. 2006; 3: 448-57.
  21. Yeh HH, Ogawa K, Balatoni J, Mukhopadhyay U, Pal A, Gonzalez-Lepera C, et al. Molecular imaging of active mutant L858R EGFR kinase-expressing non small cell lung carcinomas using PET/CT. *Proc Natl Acad Sci U S A*. 2011; 108: 1603-8.
  22. Carrasco-García E, Saceda M, Grasso S, Rocamora-Reverte L, Conde M, Gómez-Martínez A, et al. Small tyrosine kinase inhibitors interrupt EGFR signaling by interacting with erbB3 and erbB4 in glioblastoma cell lines. *Exp Cell Res*. 2011; 317: 1476-89.
  23. Stommel JM, Kimmelman AC, Ying H, Nabioullin R, Ponugoti AH, Wiedemeyer R, et al. Coactivation of receptor tyrosine kinases affects the response of tumor cells to targeted therapies. *Science*. 2007; 318: 287-90.